

In situ phase transition study of nano- and coarse-grained TiO₂ under high pressure/temperature conditions

This article has been downloaded from IOPscience. Please scroll down to see the full text article.

2008 J. Phys.: Condens. Matter 20 125224

(<http://iopscience.iop.org/0953-8984/20/12/125224>)

View [the table of contents for this issue](#), or go to the [journal homepage](#) for more

Download details:

IP Address: 129.252.86.83

The article was downloaded on 29/05/2010 at 11:10

Please note that [terms and conditions apply](#).

In situ phase transition study of nano- and coarse-grained TiO₂ under high pressure/temperature conditions

Yuejian Wang^{1,5}, Yusheng Zhao¹, Jianzhong Zhang¹, Hongwu Xu²,
Liping Wang³, Sheng-Nian Luo⁴ and Luke L Daemen¹

¹ LANSCE Division, Los Alamos National Laboratory, Los Alamos, NM 87545, USA

² EES Division, Los Alamos National Laboratory, Los Alamos, NM 87545, USA

³ Mineral Physics Institute, Stony Brook University, Stony Brook, NY 11794-2100, USA

⁴ Physics Division, Los Alamos National Laboratory, Los Alamos, NM 87544, USA

E-mail: Yuejianw@lanl.gov

Received 23 October 2007, in final form 20 December 2007

Published 3 March 2008

Online at stacks.iop.org/JPhysCM/20/125224

Abstract

A comparative phase transition study of nanocrystalline and micro-TiO₂ has been conducted under high pressure–temperature (P – T) conditions using energy-dispersive synchrotron x-ray diffraction (XRD). Our study reveals that on compression at room temperature, the micro-tetragonal anatase-type TiO₂ started to transform to the orthorhombic columbite-type TiO₂ near 1.6 GPa. In contrast, we did not observe this phase transition in nano-anatase at pressures of up to 8.5 GPa. At 8.5 GPa, by applying moderate heat, both samples were transformed completely to columbite-type TiO₂ almost simultaneously, indicating that heat treatment could significantly expedite this phase transition. These columbite-type TiO₂ phases were quenchable because after cooling them to room temperature and decompressing them to 2.0 GPa, the XRD patterns displayed no changes in comparison with those collected at 8.6 GPa and 1270 K. At 2 GPa, we heated the specimens again, and the rutile-type TiO₂ started to emerge around 970 K. This phase was also quenchable after cooling and releasing pressure to ambient conditions. The grain size effects on the phase transition were discussed based on the kinetics mechanism. This study should be of considerable interest to the fields of materials science and condensed matter.

(Some figures in this article are in colour only in the electronic version)

1. Introduction

Three distinct polymorphs, anatase (tetragonal, space group $I4_1/amd$, PDF#841285, lattice parameters: $a = 3.784$, $c = 9.512$), rutile (tetragonal, space group $P4_2/mnm$, PDF#820514, lattice parameters: $a = 4.508$, $c = 3.027$), and brookite (orthorhombic, space group $Pbca$, PDF#761937, lattice parameters: $a = 9.211$, $b = 5.472$, $c = 5.171$), of titanium dioxide (TiO₂) are known to occur in nature. Other structures such as columbite (orthorhombic α -PbO₂-type, space group $Pbcn$, PDF#841750; lattice parameters: $a = 4.531$, $b = 5.501$, $c = 4.906$) and baddeleyite (monoclinic ZrO₂-type, space group $P2_1/c$, PDF#481278;

lattice parameters: $a = 4.64$, $b = 4.76$, $c = 4.81$, $\beta = 99.2$) may be stable but only at high pressure. The high-pressure polymorphism of TiO₂ has been intensively studied over the last four decades; however, most of the previous experiments were performed at room temperature, with the Raman spectroscopic technique as a major tool [1–14]. Columbite-type TiO₂ was first discovered by Dacheille and Roy, when a starting anatase was compressed at pressures greater than 1 GPa, [8] and the structure was identified by Bendeliani *et al* [9]. Subsequently, numerous experiments confirmed the existence of a columbite-type TiO₂ phase at high pressure. However, the reported transition pressures range from 2.6 to 7.0 GPa, [1–7] depending on whether the sample is single-crystal or polycrystalline and how big the particle

⁵ Author to whom any correspondence should be addressed.

is. This behavior suggests a tremendous particle size effect on the phase stability of anatase. Recently, Swamy *et al* [10] found that at room temperature, the anatase nanocrystals with diameters smaller than 12 nm remained stable to ~ 20 GPa, and then were transformed to an amorphous phase at higher pressures. On the other hand, for crystals larger than 40–50 nm, anatase was transformed directly to columbite-type TiO_2 . The reversal of the normal relative thermodynamic stability between TiO_2 polymorphs and the stabilization of the amorphous phase at high pressure have been ascribed to the increased surface area contribution to the Gibbs free energy in nanocrystalline materials [11, 12].

Even though there have been several investigations on the high-temperature behavior of nanocrystalline TiO_2 , the significant crystal growth during the sintering process makes it difficult to elucidate the role of nanocrystal size on the temperature-induced phase transition. [13–15] The simultaneous high P – T technique provides a unique and efficient way to discern the size effect on transition temperature, because the crystal growth is typically accompanied by long-range atomic rearrangements and is therefore kinetically hindered by external pressure. Furthermore, the phase-evolution study of nanocrystalline/microcrystalline TiO_2 in a single experiment enables us to eliminate the systemic errors arising from the instrument response and pressure/stress determination. Thus, this approach allows detections of minute differences between nano- and micro-phases as well as evaluation of the finite-size effect on phase transitions [16–18].

2. Experimental details and method for grain size estimation

High-purity (>99%) nanocrystalline and microcrystalline anatase powders were purchased from Sigma-Aldrich. The powders have a grain size distribution of 4–8 nm and 40–50 μm , respectively. The energy-dispersive synchrotron XRD measurements were carried out using a cubic anvil apparatus at beamline X17B2 of the National Synchrotron Light Source (NSLS), Brookhaven National Laboratory (BNL). A mixture of amorphous boron and epoxy resin was used as the pressure medium, and a graphite tube was used as the heating furnace. The nano- and micro-anatase samples were packed into a cylindrical boron-nitride (BN) container, separated by a layer of NaCl powders, which was used as an internal pressure standard. The detailed description of the cell assembly preparation and the simultaneous study of two or more samples in a single high-pressure experiment using synchrotron XRD were elaborated in [17] and [19]. The sample pressure was determined using the Decker equation-of-state [20] for sodium chloride (NaCl). The temperature was measured directly by a W/Re25%–W/Re3% thermocouple placed at the center of the pressure cell. At the end of the experiment, NaCl, which was also used to calibrate the diffraction Bragg angle, was recovered with its initial unit-cell parameter within errors of the refinements, indicating no changes in system calibration (i.e. Bragg angle) over the entire experimental P – T range. The P – T path of the whole run is shown in figure 1.

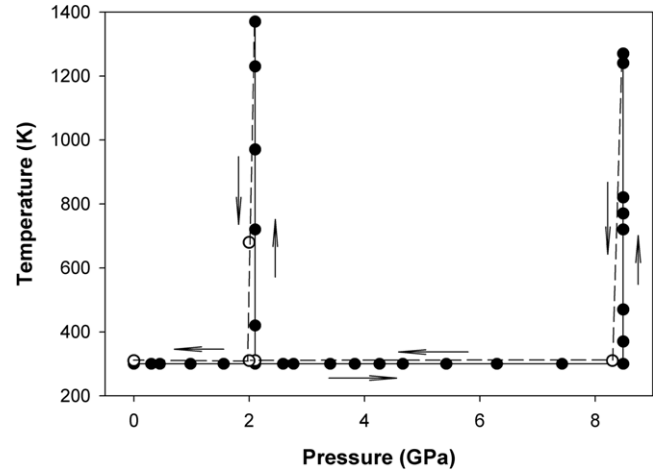


Figure 1. P – T paths for the synchrotron XRD experiments. The solid circles connected with the solid lines represent the heating-compression paths, and the hollow circles linked by the dashed lines correspond to the cooling-decompression routes. The experiments began with the ambient condition. We increased the pressure by steps up to 8.5 GPa and then heated the samples to each desired temperature. After reaching 1270 K, we first reduced the sample temperature to room temperature and afterwards released the pressure to 2 GPa, at which point a new heating-cooling cycle started. In this cycle, we kept the constant loading force and increased the temperature in steps to the maximum value of 1370 K, and finally returned the P – T to ambient condition. The experimental directions are indicated by arrows in the figure. Points corresponding to the same P – T of compression and decompression cycles are arbitrarily offset to guide the eyes.

The grain sizes were estimated from peak width analysis of XRD profiles. Following our previous work [21, 22], we express the FWHM of diffraction peaks on a length scale of angstrom (\AA), Δd (FWHM), which can be used to quantify differential strain (ε) introduced by stress heterogeneity, lattice deformation, and dislocation density at high P – T . They can also be used to quantify the contributions of instrument response and grain sizes of polycrystalline materials, in the form of

$$\Delta d_{\text{obs}}^2/d^2 = (\varepsilon^2 + \Delta d_{\text{ins}}^2/d^2) + (\kappa/L)^2 \cdot d^2(P, T). \quad (1)$$

Here, Δd_{obs} and Δd_{ins} are the observed peak width and the peak width at a stress-free state, respectively, d is the d -spacing of a given lattice plane, L the material's grain size, and κ the Scherer constant. Equation (1) is a typical $Y = \mathbf{a} + \mathbf{b} \cdot X$ plot. Therefore, one can derive the apparent strain $\varepsilon_{\text{apparent}}^2 = (\varepsilon^2 + \Delta d_{\text{ins}}^2/d^2)$ as well as average grain size L from the ordinate intercept and slope of the $\Delta d_{\text{obs}}^2/d^2$ versus $d^2(P)$ plot, respectively.

3. Results and discussion

The XRD patterns for nano-/micro-anatase simultaneously compressed at room temperature are shown in figure 2. At each identical pressure condition, the diffraction peaks of nano-anatase are broader than those of micro-anatase. At ambient conditions, the triplet peaks A (112), (004), and (103) of

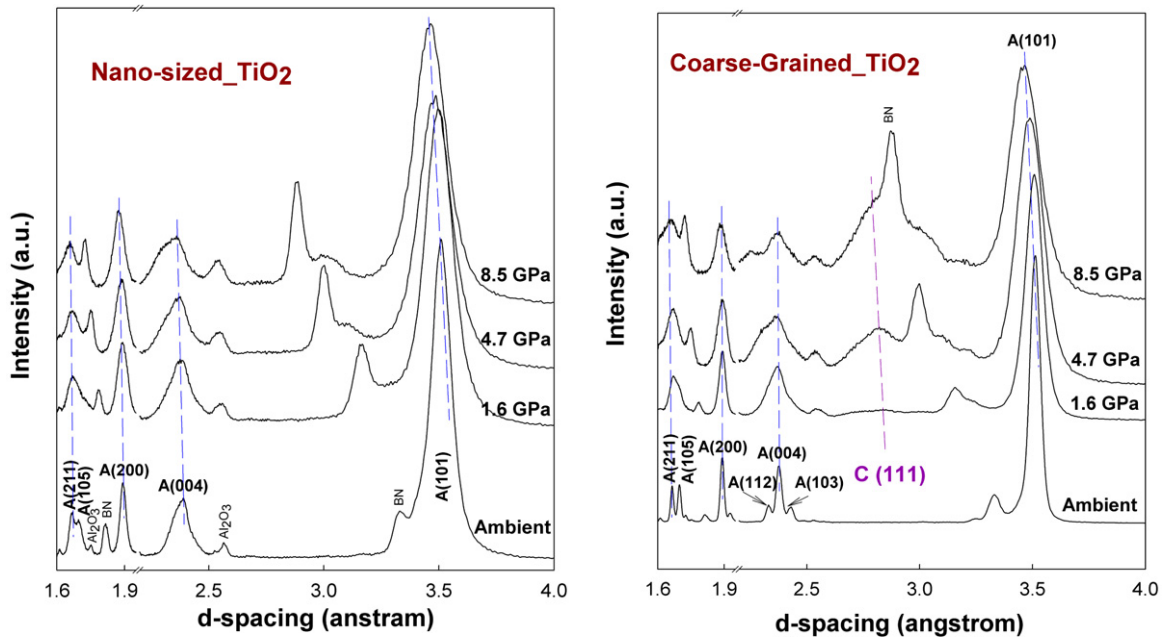


Figure 2. Selected XRD patterns as the samples were compressed at room temperature. The left set of patterns is for the nano-TiO₂ and the right set for micro-TiO₂. The letters A and C refer to anatase and columbite-type TiO₂, respectively. The green and pink dashed lines are to identify the identical peaks under various pressures. Some peaks are from the boron–nitride (BN) capsule and the alumina (Al₂O₃) sleeve of the cell assembly.

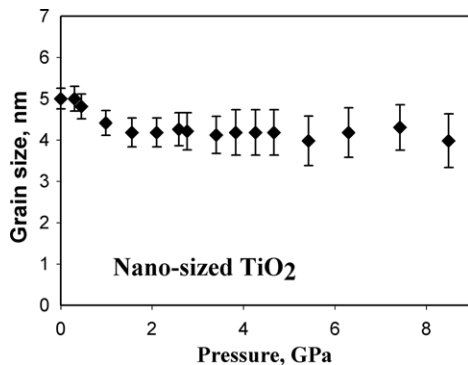


Figure 3. The grain size variation of nano-anatase during compression at room temperature. Vertical bars refer to the uncertainties associated with the grain size determination.

micro-anatase are clearly distinguishable; however, for nano-anatase, all three peaks overlap, resulting in a single, broad peak. This initial significant peak broadening of nano-anatase primarily results from its small particle size effect. With increasing pressure, the diffraction peaks of both samples become continuously more broadened. XRD line-broadening analysis revealed that the grain size of nano-TiO₂ remains essentially constant at pressures up to 8.5 GPa (figure 3). Upon heating at 8.5 GPa, the grain size stays unchanged up to the temperature of the anatase–columbite transition (~ 473 K). For bulk TiO₂, the grain size variation could not be accurately measured due to the limitation of detector resolution; the analysis, however, shows that the slopes in the $\Delta d^2/d^2-d^2$ plots are either close to zero or negative values, indicating that the grain size is still within the micron-size regime throughout

the experiment. These analyses suggest that the observed peak broadening is primarily caused by the severe contact stresses applied on the crystal grains at high pressure.

Another prominent change is the pressure-induced phase transition from micro-anatase to columbite-type TiO₂, which started near 1.6 GPa. The transition process, however, was so sluggish that it did not complete even when the pressure was elevated to 8.5 GPa. In contrast, no phase transition was observed in the nanosized counterpart. Careful comparison of the two sets of XRD patterns show new peaks for the coarse-grained anatase, which can be indexed as the columbite-type TiO₂ peak (111). Retaining structure integrity in nano-anatase at high pressure is in fairly good agreement with the previous experimental observations. However, the onset pressure for the anatase-to-columbite transition (1.6 GPa) observed in this study for micron-TiO₂ is lower than those reported in the literature [1–7].

There have been several attempts to explain the striking phase stability of nano-anatase at high pressure. Hearne *et al* [1] demonstrated that there exists a critical particle diameter (threshold size), d^* , for self-sustaining growth of the nucleus of columbite-type TiO₂. In the case of the nanocrystalline anatase, because its crystal size is smaller than d^* , it would require additional energy to transform it to a new phase. In other words, nano-anatase is energetically favorable to persist at high pressure. Wang [23] suggested that the high surface energy, associated with the high concentration of grain boundaries, might stabilize TiO₂ in the starting anatase phase. Recently, based on the so-called ‘apparent lattice parameter (alp)’, Palosz and his co-workers [24, 25] proposed a new approach to evaluate the structures of nanocrystals. In this model, nanoparticles are treated as having a complicated

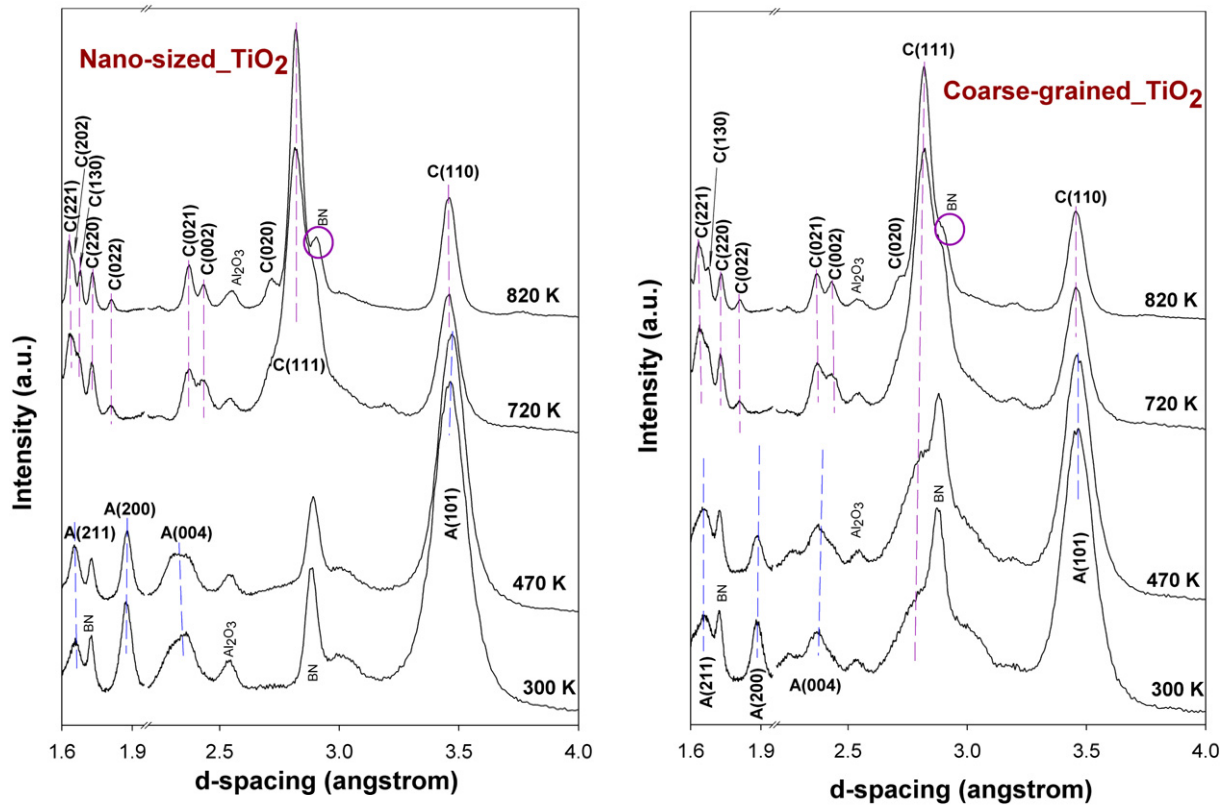


Figure 4. Selected XRD patterns plotted as a function of heating temperature for nano-TiO₂ (left panel) and micro-TiO₂ (right panel) at 8.5 GPa. The pink circles in the patterns show the different peak broadenings of specimens under high-temperature treatment at 8.5 GPa.

core-shell structure, and the number of atoms residing on the surface shell can exceed the number of atoms in the core. Therefore, for nanocrystals, the grain boundaries and surface atoms dominate the properties of the entire material. Under stress, the surface shell is more compressible than the core, thereby forming a strong network of grain boundaries with a matrix tightly embedded with the grain core. The compressed and shrunk shell leads to high surface energy of a nanocrystal, which would hinder the phase transformation. For coarse-grained materials showing a perfectly periodic order in an infinite crystal lattice, under high pressure all the atoms in a grain would equally accommodate the applied external stress, and, therefore, the surface energy is lower than that of nanosized materials. This lower surface energy of coarse-grained materials under stress may easily give rise to the phase transition at a relatively low pressure.

The diffraction patterns shown in figure 4 are selected to display the peak profile variations and phase transformations of the samples when subject to a heating treatment at 8.5 GPa. For nano-anatase, no columbite-type TiO₂ was formed below 473 K, but the columbite-type TiO₂ phase in the coarse-grained specimen grows steadily with increasing temperature. Upon heating to 720 K, both specimens were transformed completely to the columbite-type TiO₂ phase. It should be noted that during heating, the temperature showed a sudden and abnormal increase from 473 to 720 K, which is most likely caused by the phase-transition-induced changes in the heater's geometry and therefore its electrical resistance. Therefore, it is

reasonable to assume that the onset temperature for the anatase to columbite-type TiO₂ transition in nano-TiO₂ is closer to 473 K than to 720 K. At further higher temperatures, the diffraction peaks in both nano- and micro-columbite-type TiO₂ became progressively narrower. At a given temperature, the columbite-type TiO₂ transformed from nano-anatase shows sharper peaks than that transformed from micro-anatase. For example, C (111) is fully overlapped with one BN peak in the case of coarse-grained anatase; however, for nanosized anatase, the upper segments of the two peaks are well resolved, as illustrated by the pink circles in figure 3. After reaching the highest temperature, 1270 K, the samples were cooled to room temperature and then decompressed to 2 GPa, under which both patterns had no obvious changes and were similar to those at 1270 K and 8.3 GPa.

It should be noted that the observed transition pressure of 1.6 GPa for micron-TiO₂ at 300 K and 8.5 GPa for nano-TiO₂ at ~473 GPa can only provide the upper bounds for their respective equilibrium transition pressures. This is because nucleation in solid-state polymorphic phase transformations is typically accompanied by the creation of the interface between new and original phases, which requires additional energy. Furthermore, for transformation occurring at high pressures, the new phase usually has a different density. This misfit creates elastic stresses around nuclei and also consumes some energy. As a result, the phase transformation cannot start immediately at the equilibrium phase boundary but only after some metastable overshoot in pressure (ΔP), which provides a

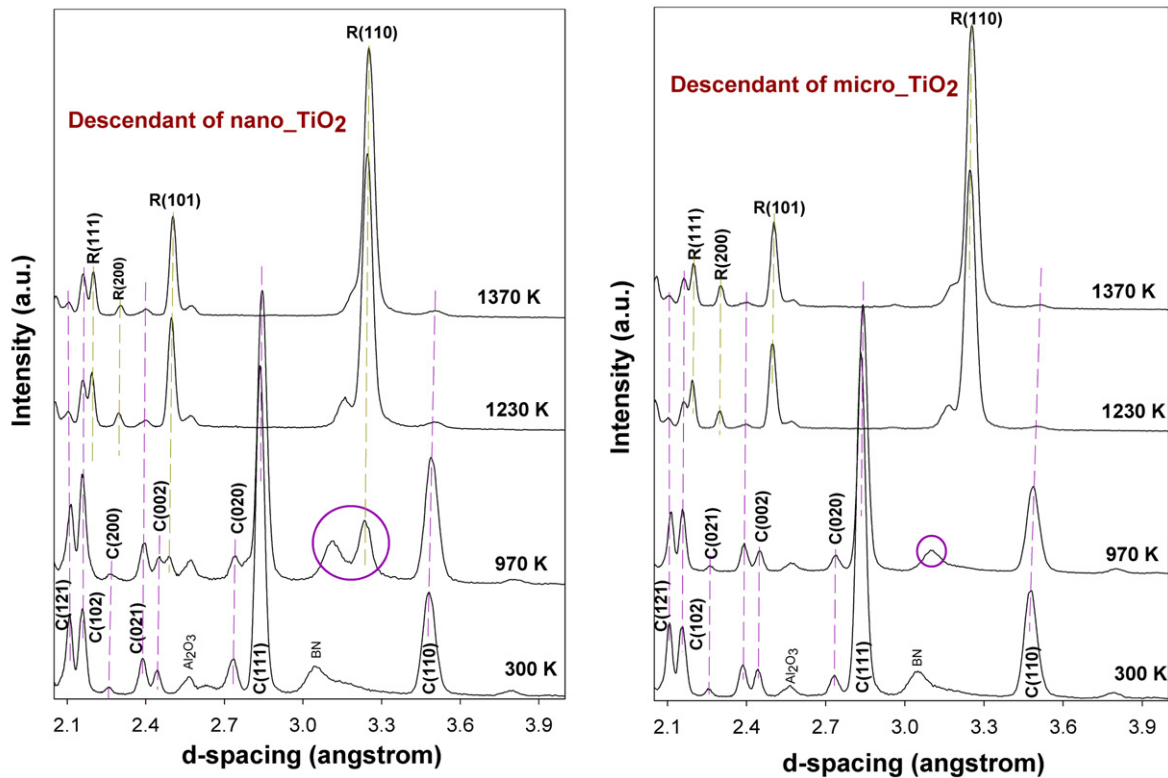


Figure 5. High-temperature XRD patterns (left: the descendant of nanosized TiO_2 , right: the descendant of micro- TiO_2) at 2.0 GPa. R denotes rutile. The pink circles in the figures illustrate the discrepancy in phase evolutions of two specimens at 970 K.

sufficiently large driving force (ΔG) to overcome a nucleation barrier for transformation to occur. The driving force is described by $\Delta G = \Delta V \Delta P$, where ΔV is the volume change upon transformation and ΔP the difference between the observed pressure of the phase transformation and the pressure at equilibrium for a given temperature, also referred to as the nucleation barrier of the transformation [26]. The present study shows that the nucleation barrier is substantially increased for the anatase-to-columbite transition when grain size is reduced to less than 10 nm, which can be attributed to the additional surface energy in nanocrystalline TiO_2 .

At high temperatures, the stress relaxation and corresponding rearrangement of atoms, which leads to lower surface energy of nanocrystals and increased atomic mobility, are predominately responsible for the temperature-induced phase transition. Other factors also contribute to this progress. For example, large surface-to-volume ratio, high defect concentration, and a large portion of atoms residing in the surface shell may abruptly promote the phase transition and accelerate the new phase growth when the temperature reaches a certain height and the surface energy drops to a low-enough level. From the inspection of XRD patterns of nano-anatase at 470 and 300 K, the progressively narrowing peaks are dominantly due to the stress relaxation. As the elevated temperature exceeding the critical temperature of 470 K, however, the grain growth of a new phase contributes significantly to the peak sharpening.

In order to characterize other temperature-induced phase transitions involving the newly formed columbite-type TiO_2 ,

a heating-cooling run at 2 GPa was conducted, and the representative XRD patterns are depicted in figure 5. After the high P - T treatment, it is inappropriate to distinguish the two samples by the grain size of their source materials because there is no direct correspondence between the sizes of starting and ending materials. Here, we name the phase evolved from nano-anatase as the descendant of nano-anatase, and that from the micro-anatase as the descendant of coarse-grained anatase. Although both samples transformed to rutile on heating, their onset temperatures of the transition were different. As indicated by the pink circles in the figures, the descendant of nano-anatase started to transform to rutile at 970 K or even lower; however, in contrast, there was no phase transition observed at this temperature in the descendant of the coarse-grained anatase. The transition process did not complete at the highest temperature 1370 K, and there always coexisted some amounts of columbite-type TiO_2 and rutile. Finally, like the above-mentioned columbite-type TiO_2 , rutile is also quenchable to ambient conditions. The fact that x-ray patterns of two samples at 2 GPa and 300 K show no noticeable difference indicates that after experiencing high P - T treatment, the nanograin grows to micrometer sizes. In this case, therefore, the size effect does not explain the different onset temperature of phase transition from columbite-type TiO_2 to rutile. The exact mechanism resulting in this discrepancy is not fully understood yet.

In summary, using the *in situ* synchrotron XRD, we have provided a detailed phase-evolution characterization of nano-/micro-anatase in a single high P - T experiment. Our

results indicate that the particle size is an important factor in controlling the phase stability of nanocrystalline anatase. At room temperature, nano-anatase maintains its stable structure to high pressure, in contrast with the phase transition of micro-anatase to columbite-type TiO₂ at 1.6 GPa. The complex shell-core structure of nanocrystalline anatase that has high surface energy under stress may restrain its phase transition. However, high-temperature treatment that intensifies the kinetics and atomic mobility of nano-anatase, thus abruptly promotes the nano-anatase → columbite-type TiO₂ transition. After further high *P*–*T* treatment, nanograins grow in micrometer sizes, and both samples do not exhibit a striking difference, except for the different onset phase transition temperature from columbite-type TiO₂ to rutile. Furthermore, our results reveal that both columbite-type TiO₂ and rutile transformed in turn from anatase under high *P* and *T* are quenchable to ambient conditions.

Acknowledgments

This research is supported by the Los Alamos National Laboratory, which is operated by Los Alamos National Security LLC under DOE Contract DE-AC52-06NA25396. The experimental work was carried out at the beamline X17B2 of National Synchrotron Light Source, Brookhaven National Laboratory, which is supported by the Consortium for Materials Properties Research in Earth Sciences (COMPRES) under NSF Cooperative Agreement EAR 01-35554.

References

- [1] Hearne G R, Zhao J, Dawe A M, Pischedda V, Maaza M, Nieuwoudt M K, Kibasomba P, Nemraoui O, Comins J D and Witcomb M 2004 *J. Phys. Rev. B* **70** 134102
- [2] Ohsaka T, Yamaoka S and Shimomura O 1979 *Solid State Commun.* **30** 345
- [3] Haines J and Leger J M 1993 *Physica B* **192** 233
- [4] Lagarec K and Desgreniers S 1995 *Solid State Commun.* **94** 519
- [5] Arlt T, Beermejo M, Blanco M A, Gerward L, Jiang J, Olsen J S and Recio J M 2000 *Phys. Rev. B* **61** 14414
- [6] Olsen J S, Gerward L and Jiang J 1999 *J. Phys. Chem. Solids* **60** 229
- [7] Swamy V, Dubrovinsky L S, Dubrovinskaia N A, Simionovici A S, Drakopoulos M, Dmitriev V and Weber H P 2003 *Solid State Commun.* **125** 111
- [8] Dachille F and Roy R 1962 *Am. Ceram. Soc. Bull.* **41** 225
- [9] Bendeliani N A, Popova S V and Vereshchagin L F 1966 *Geochem. Int.* **3** 387
- [10] Swamy V, Kuznetsov A, Dubrovinsky L S, Caruso R A, Shchukin D G and Muddle B C 2005 *Phys. Rev. B* **71** 184302
- [11] Navrotsky A 2003 *Geochem. Trans.* **4** 34
- [12] McHale J M, Auroux A, Perrotta A J and Navrotsky A 1997 *Science* **277** 788
- [13] Edelson L H and Glaeser A M 1998 *J. Am. Ceram. Soc.* **71** 225
- [14] Kumar K P, Keizer K and Burggraaf A J 1993 *J. Mater. Chem* **3** 917
- [15] Sheinkman A I, Tymentsev V A and Fotiev A A 1985 *J. Mater. Chem.* 1460
- [16] Hazen R M 1993 *Science* **259** 206
- [17] Zhang J and Kostak P 2002 *Phys. Earth Planet. Inter.* **129** 301
- [18] Zhang J, Zhao Y and Palosz B 2007 *Appl. Phys. Lett.* **90** 043112
- [19] Vaughan M T, Weidner D J, Wang Y, Chen J, Koleda C C and Getting I C 1998 *Rev. High Pressure Sci. Technol.* **7** 1520
- [20] Decker D L 1971 *J. Appl. Phys.* **42** 3239
- [21] Zhao Y, Zhang J, Clausen B, Shen T D, Gray G T III and Wang L 2007 *Nano Lett.* **7** 426
- [22] Wang Y, Zhang J and Zhao Y 2007 *Nano Lett.* **7** 3196
- [23] Wang Z, Saxena S K, Pischedda V, Liermann H P and Zha C 2001 *J. Phys.: Condens. Matter* **13** 8317
- [24] Palosz B, Stelmakh S, Grzanka E, Gierlotka S, Pielaszek R, Bismayer U, Werner S and Palosz W 2004 *J. Phys.: Condens. Matter* **16** S353
- [25] Palosz B, Grzanka E, Gierlotka S, Stelmakh S, Pielaszek R, Bismayer U, Neufeind J, Weber H P and Palosz W 2002 *Acta Phys. Pol. A* **102** 57
- [26] Zhang J, Zhao Y, Pantea C, Qian J, Rigg P, Hixson R, Gray G T, Yang Y, Wang L and Wang Y 2005 *J. Phys. Chem. Solids* **66** 1213